
This is an electronic reprint of the original article.
This reprint may differ from the original in pagination and typographic detail.

Garde, Henrik; Hirvensalo, Markus

Linearized Calderón Problem: Reconstruction of Unbounded Perturbations in Three Dimensions

Published in:
SIAM Journal on Applied Mathematics

DOI:
[10.1137/24M1649162](https://doi.org/10.1137/24M1649162)

Published: 01/01/2025

Document Version
Publisher's PDF, also known as Version of record

Please cite the original version:
Garde, H., & Hirvensalo, M. (2025). Linearized Calderón Problem: Reconstruction of Unbounded Perturbations in Three Dimensions. *SIAM Journal on Applied Mathematics*, 85(1), 210-223.
<https://doi.org/10.1137/24M1649162>

LINEARIZED CALDERÓN PROBLEM: RECONSTRUCTION OF UNBOUNDED PERTURBATIONS IN THREE DIMENSIONS*

HENRIK GARDE[†] AND MARKUS HIRVENSAALO[‡]

Abstract. Recently, an algorithm was given in Garde and Hyvönen [*SIAM J. Math. Anal.*, 56 (2024), pp. 3588–3604] for exact direct reconstruction of any L^2 perturbation from linearized data in the two-dimensional linearized Calderón problem. It was a simple forward substitution method based on a two-dimensional Zernike basis. We now consider the three-dimensional linearized Calderón problem in a ball and use a three-dimensional Zernike basis to obtain a method for exact direct reconstruction of any L^3 perturbation from linearized data. The method is likewise a forward substitution, hence making it very efficient to numerically implement. Moreover, the three-dimensional method only makes use of a relatively small subset of boundary measurements for exact reconstruction compared to a full L^2 basis of current densities.

Key words. Calderón problem, linearization, reconstruction, three-dimensional Zernike basis

MSC codes. 35R30, 35R25

DOI. 10.1137/24M1649162

1. Introduction. Let B be the unit ball in \mathbb{R}^3 . For a conductivity coefficient $\gamma \in L^\infty(B; \mathbb{R})$, with $\text{essinf } \gamma > 0$, and a surface current density

$$f \in L^2_\diamond(\partial B) = \{g \in L^2(\partial B) \mid \langle g, 1 \rangle_{L^2(\partial B)} = 0\},$$

the continuum model for the conductivity problem states that the corresponding interior electric potential u satisfies

$$(1.1) \quad -\nabla \cdot (\gamma \nabla u) = 0 \text{ in } B, \quad \nu \cdot (\gamma \nabla u) = f \text{ on } \partial B,$$

where ν is the exterior unit normal. The Lax–Milgram lemma yields a unique solution u_f^γ to (1.1) in the space

$$H^1_\diamond(B) = \{w \in H^1(B) \mid w|_{\partial B} \in L^2_\diamond(\partial B)\}.$$

The Neumann-to-Dirichlet (ND) map $\Lambda(\gamma)f = u_f^\gamma|_{\partial B}$ is a compact self-adjoint operator in the space $\mathcal{L}(L^2_\diamond(\partial B))$, mapping any applied current density to the corresponding boundary potential measurement.

The nonlinear forward map $\gamma \mapsto \Lambda(\gamma)$ is Fréchet differentiable with respect to complex-valued perturbations $\eta \in L^\infty(B)$. Let $F = D\Lambda(1; \eta)$ be the Fréchet derivative of Λ at $\gamma \equiv 1$ with respect to perturbation η . If u_f and u_g are harmonic functions in B

*Received by the editors March 25, 2024; accepted for publication October 28, 2024; published electronically January 28, 2025.

<https://doi.org/10.1137/24M1649162>

Funding: The work of the first author was supported by Independent Research Fund Denmark, Natural Sciences (grant 10.46540/3120-00003B). The work of the second author was supported by the Academy of Finland (decisions 353081 and 359181).

[†]Department of Mathematics, Aarhus University, 8000 Aarhus C, Denmark (garde@math.au.dk).

[‡]Department of Mathematics and Systems Analysis, Aalto University, 00076 Helsinki, Finland (markus.hirvensalo@aalto.fi).

with f and g as their Neumann traces, respectively, then $F \in \mathcal{L}(L^\infty(B), \mathcal{L}(L^2_\diamond(\partial B)))$ is characterized by

$$(1.2) \quad \langle (F\eta)f, g \rangle_{L^2(\partial B)} = - \int_B \eta \nabla u_f \cdot \overline{\nabla u_g} \, dx$$

for $\eta \in L^\infty(B)$ and $f, g \in L^2_\diamond(\partial B)$. The linearized Calderón problem is

$$\text{Reconstruct } \eta \text{ from knowledge of } F\eta.$$

This is in contrast to the (nonlinear) Calderón problem to reconstruct a coefficient γ from $\Lambda(\gamma)$.

By Proposition A.1, F continuously extends to an operator acting on perturbations in the larger space $L^3(B) \supset L^\infty(B)$, hence allowing for unbounded perturbations. Generally, for a bounded smooth domain Ω in \mathbb{R}^d , F extends to perturbations in $L^d(\Omega)$. For the extension result, it is important that the Neumann conditions are in L^2 and not, e.g., $H^{-1/2}$. This indicates that it may be possible to generalize the two-dimensional reconstruction method in [10] to three spatial dimensions but for general perturbations in L^3 instead of L^2 . The technique from [10] for obtaining stability for infinite-dimensional spaces of perturbations, however, is out of reach, as we cannot make use of the Hilbert–Schmidt topology in three spatial dimensions as outlined in [10, section 1.3] and [9, Appendix A].

Calderón’s original injectivity proof for the linearized problem directly extends to $L^3(B)$, showing that $F\eta$ vanishes identically if and only if the Fourier transform for η (zero-extended to \mathbb{R}^3) vanishes [4]. See also [7, 8, 16, 17] for additional uniqueness results in the linearized Calderón problem, including the case of partial data [7, 17].

In spherical coordinates, with radial distance r , polar angle θ , and azimuthal angle φ , the three-dimensional Zernike basis functions are

$$(1.3) \quad \psi_\ell^{k,m}(r, \theta, \varphi) = R_\ell^k(r) Y_\ell^m(\theta, \varphi), \quad k, \ell \in \mathbb{N}_0, \quad m \in \mathbb{Z}_\ell,$$

where

$$\mathbb{Z}_\ell = \{-\ell, \dots, \ell\}.$$

Here Y_ℓ^m are the spherical harmonics of degree ℓ and order m , and R_ℓ^k are three-dimensional radial Zernike polynomials (see section 3 for definitions and notation). $\{\psi_\ell^{k,m}\}_{\ell, k \in \mathbb{N}_0, m \in \mathbb{Z}_\ell}$ is an orthonormal basis for $L^2(B)$ by Proposition 3.2, which we will use for expanding a perturbation $\eta \in L^3(B) \subset L^2(B)$.

Any $\eta \in L^3(B)$ can be reconstructed from the linearized data $F\eta$ via our main result below.

THEOREM 1.1. *For any $\eta \in L^3(B)$ expanded as*

$$\eta = \sum_{k \in \mathbb{N}_0} \sum_{\ell \in \mathbb{N}_0} \sum_{m \in \mathbb{Z}_\ell} c_\ell^{k,m} \psi_\ell^{k,m}$$

for an ℓ^2 -sequence of coefficients $c_\ell^{k,m}$,

$$c_\ell^{k,m} = (Q_{\ell,0}^{k,m,k})^{-1} \left(\langle (F\eta) Y_{k+1}^0, Y_{\ell+k+1}^m \rangle_{L^2(\partial B)} - \sum_{q=0}^{k-1} \sum_{s=0}^{k-q} Q_{\ell,s}^{k,m,q} c_{\ell+2s}^{q,m} \right).$$

The scalars $Q_{\ell,s}^{k,m,q}$ are independent of η and defined as

$$Q_{\ell,s}^{k,m,q} = (-1)^{m+1} \frac{\sqrt{2\ell+4q+4s+3}(k-s+1)(k-q-s+1)_q}{(k+1)(\ell+k+1)(\ell+k+s+\frac{5}{2})_q} G_{k+1,\ell+k+1,\ell+2s}^{0,-m,m}$$

using Pochhammer symbols (rising factorials) and the Gaunt coefficient

$$G_{k+1,\ell+k+1,\ell+2s}^{0,-m,m} = \int_{\partial B} Y_{k+1}^0 Y_{\ell+k+1}^{-m} Y_{\ell+2s}^m dS.$$

The reason for leaving the Gaunt coefficient in $Q_{\ell,s}^{k,m,q}$ instead of inserting its exact value from (3.4) is that Gaunt coefficients can be efficiently computed using finite element (FE) methods or using direct implementations in libraries such as SymPy.

If we let

$$\eta_k = \sum_{\ell \in \mathbb{N}_0} \sum_{m \in \mathbb{Z}_\ell} c_\ell^{k,m} \psi_\ell^{k,m},$$

then η_k is an orthogonal projection of η onto a particular infinite-dimensional subspace of $L^2(B)$, with $k=0$ giving the subspace of harmonic functions. Since

$$\eta = \sum_{k \in \mathbb{N}_0} \eta_k,$$

Theorem 1.1 implies that we can inductively reconstruct η one orthogonal projection at a time. We have that η_0 , i.e., the coefficients $\{c_\ell^{0,m}\}_{\ell \in \mathbb{N}_0, m \in \mathbb{Z}_\ell}$, is directly reconstructed from the data $(F\eta)Y_1^0$. Next, η_1 , i.e., the coefficients $\{c_\ell^{1,m}\}_{\ell \in \mathbb{N}_0, m \in \mathbb{Z}_\ell}$, is directly reconstructed from the data $(F\eta)Y_2^0$ and η_0 . In general, we have that η_k is directly reconstructed from $(F\eta)Y_{k+1}^0$ and $\eta_0, \dots, \eta_{k-1}$. Moreover, if one considers only finite measurements $\{(F\eta)Y_{k+1}^0\}_{k=0}^K$, then the formula in Theorem 1.1 still provides the exact reconstruction of the orthogonal projections η_0, \dots, η_K due to the method essentially being a forward substitution.

Theorem 1.1 is the three-dimensional variant of the two-dimensional reconstruction method in [10, Theorem 1.3], which made use of a two-dimensional Zernike basis [18] to obtain a very similar triangular structure for the solution formulas of the coefficients. We note the interesting fact that in three spatial dimensions, fewer data are required for the reconstruction in the sense that the current densities Y_{k+1}^0 applied for the measurements do not vary in the m -index of the spherical harmonics. If all Y_ℓ^m spherical harmonics are used as current densities in the measurements, then there would be an enormous redundancy since the range of m -indices grows as $2\ell+1$. This is unlike in two spatial dimensions, where all the Fourier basis functions are used.

Another difference from the two-dimensional method is that the three-dimensional method is likely less numerically stable since there is an extra sum where previously computed coefficients are needed with a higher ℓ -index than the $c_\ell^{k,m}$ that is being reconstructed. This comes from the fact that the product of two exponentials is once again an exponential, and the additional sum therefore does not appear in two spatial dimensions by orthogonality in the Fourier basis. However, in three spatial dimensions, the product of two spherical harmonics is a finite linear combination of spherical harmonics of various degrees. Nevertheless, we are still able to obtain good approximate reconstructions from inaccurate measurements.

1.1. Article structure. We give a numerical example in section 2, indicating how the inherent ill-posedness of the problem is observed in practice. Section 3 introduces the spherical harmonics, three-dimensional radial Zernike polynomials, and related results. Section 4 proves Theorem 1.1. Finally, Appendix A extends the linearized problem from perturbations in L^∞ to L^d for spatial dimension d .

2. A simple numerical example. Consider the following translated and very localized Gaussian-type perturbation:

$$(2.1) \quad \eta(x) = e^{-50|x-(0, \frac{3}{10}, 0)^T|^2} = e^{-50r^2 + 30r \sin(\theta) \sin(\varphi) - \frac{9}{2}}.$$

Figure 2.1 shows η and the sum of the real part of the first few projections η_k ,

$$(2.2) \quad \omega_K = \sum_{k=0}^K \operatorname{Re}(\eta_k),$$

where η_k is computed by evaluating inner products of η with the three-dimensional Zernike basis functions $\psi_\ell^{k,m}$, with $m \in \mathbb{Z}_\ell$ and up to a sufficiently high ℓ -index (here up to $\ell = 30$). With accurate measurements, the full reconstruction will follow the pattern seen in Figure 2.1 for increasing K .

We may use (4.2) together with Mathematica to compute very accurate simulated measurements, evaluated correctly to 16 digits. A natural way of regularizing the computations is a k -dependent truncation in the ℓ -indices and still using all $m \in \mathbb{Z}_\ell$ (see also [3] for more details in a two-dimensional setting). Thus, let

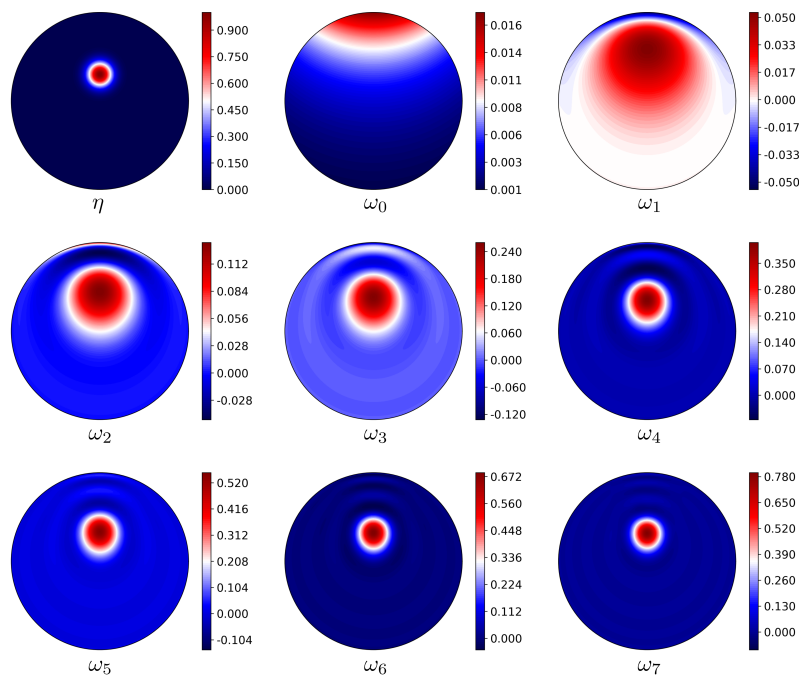


FIG. 2.1. The perturbation η from (2.1) and ω_K from (2.2) for $K = 0, \dots, 7$. The plots are in the xy -plane.

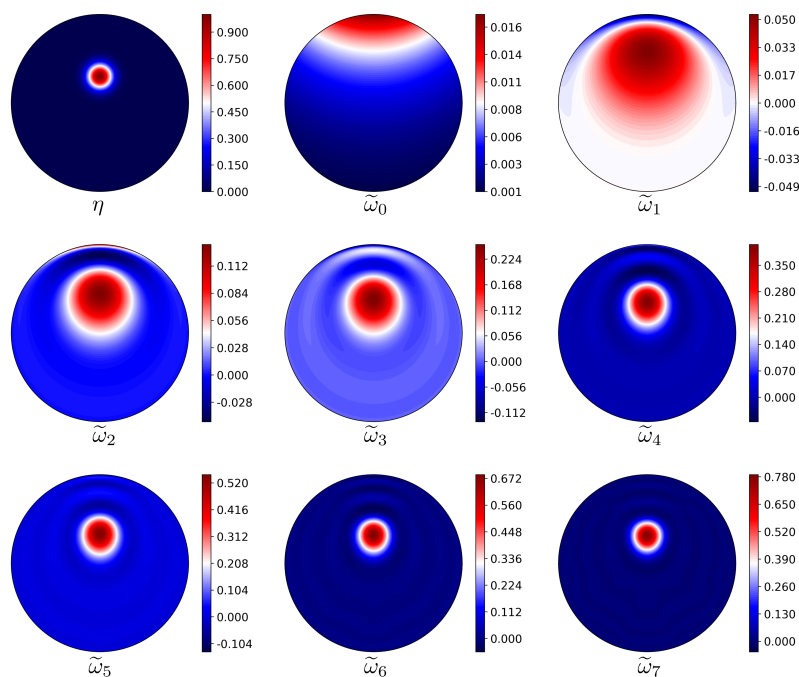


FIG. 2.2. The perturbation η from (2.1) and approximations $\tilde{\omega}_K$ from (2.3) for $K = 0, \dots, 7$ based on accurate measurements from Mathematica. The plots are in the xy -plane.

$$(2.3) \quad \tilde{\omega}_K = \sum_{k=0}^K \sum_{\ell=0}^{\ell_k} \sum_{m \in \mathbb{Z}_\ell} \operatorname{Re}(\tilde{c}_\ell^{k,m} \psi_\ell^{k,m})$$

for $K = 0, \dots, 7$ and with truncations $\ell_0 = 20$, $\ell_1 = 18$, $\ell_2 = 16$, $\ell_3 = 14$, $\ell_4 = 12$, $\ell_5 = 10$, $\ell_6 = 8$, and $\ell_7 = 6$. The approximate coefficients $\tilde{c}_\ell^{k,m}$ are found using the formula in Theorem 1.1 but with the accurate measurement data simulated in Mathematica. The results can be seen in Figure 2.2 and can be compared with Figure 2.1; the approximate reconstructions are in fact nearly perfect with the highly accurate measurements, even for the truncated indices. Indeed, the triangular nature of the method implies that the computed coefficients used for the approximate reconstructions in Figure 2.2 are *unaffected* by the truncation to a finite set of indices, which is very unique compared to other reconstruction methods.

To indicate of how this looks in a more realistic setting, with some inaccuracies in the measurements, we simulate the measurements (including numerically computing the interior electric potentials) from a rather rough FE discretization. We use \mathbb{P}_1 -elements on a tetrahedral mesh based on 6017 nodes (1026 boundary nodes) with the Python package scikit-fem [11]. The approximations are given by (2.3) for $K = 0, \dots, 4$ and with truncations $\ell_0 = 16$, $\ell_1 = 11$, $\ell_2 = 7$, $\ell_3 = 5$, and $\ell_4 = 3$. The approximate coefficients $\tilde{c}_\ell^{k,m}$ are found using the formula in Theorem 1.1 but this time with the approximate measurement data simulated by the rough FE model. The results can be seen in Figure 2.3 and can be compared with the top two rows of Figure 2.1. In practice, with noisy measurements, this is realistically what can be achieved, and these coefficients appear to be numerically quite stable to compute.

For more on numerical computations and details on regularization with this type of method, a numerical implementation of the two-dimensional method from [10],

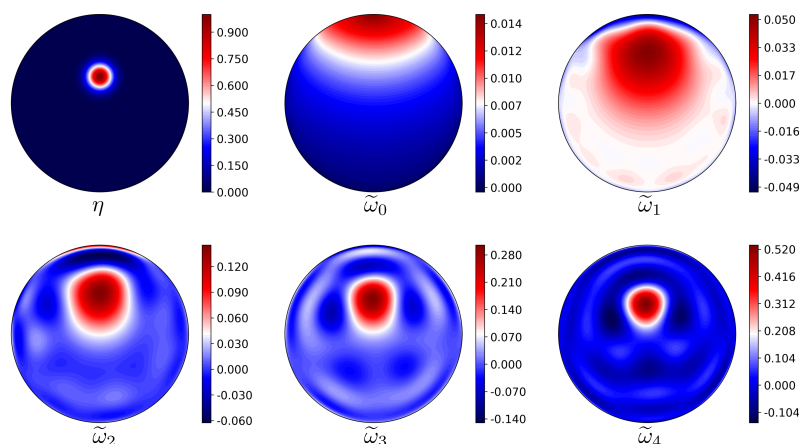


FIG. 2.3. The perturbation η from (2.1) and approximations $\tilde{\omega}_K$ from (2.3) for $K = 0, \dots, 4$ based on measurements from a rough FE model. The plots are in the xy -plane.

taking the triangular structure into account, can be found in [3]. Even for truncated difference-data $\Lambda(1 + \eta) - \Lambda(1)$, rather than linearized data, the (regularized) method consistently produces decent reconstructions. This can even be seen for data coming from practical electrode models, such as the complete electrode model, and for real-world measurements in an essentially two-dimensional measurement setup. See also [1] for a numerical study using a two-dimensional Zernike basis.

3. Constructing the three-dimensional Zernike orthonormal basis. This section defines spherical harmonics and three-dimensional radial Zernike polynomials and elaborates on related results needed for proving Theorem 1.1.

3.1. On spherical harmonics. We recall some facts about spherical harmonics; see [2, Chapter 5] and [6] for additional insights. See also [13, section 34] for more info on Wigner $3j$ symbols.

A homogeneous polynomial $p : \mathbb{R}^3 \rightarrow \mathbb{C}$ of degree ℓ (here in three spatial dimensions) satisfies $p(\lambda x) = \lambda^\ell p(x)$ for any $\lambda \in \mathbb{R}$ or, equivalently,

$$p(x) = \sum_{|\alpha|=\ell} c_\alpha x^\alpha$$

for coefficients $c_\alpha \in \mathbb{C}$ with $\alpha \in \mathbb{N}_0^3$. Multi-index notation is used, where for $\alpha \in \mathbb{N}_0^3$, we have $x^\alpha = x_1^{\alpha_1} x_2^{\alpha_2} x_3^{\alpha_3}$ and $|\alpha| = \alpha_1 + \alpha_2 + \alpha_3$. Let

$$\mathcal{A}_\ell = \left\{ p : \mathbb{R}^3 \rightarrow \mathbb{C} \mid p(x) = \sum_{|\alpha|=\ell} c_\alpha x^\alpha, c_\alpha \in \mathbb{C}, \Delta p = 0 \right\}$$

be the space of *harmonic* homogeneous polynomials of degree ℓ .

The space of spherical harmonics of degree ℓ is defined as the restriction of the harmonic homogeneous polynomials of degree ℓ to the unit sphere:

$$\mathcal{H}_\ell = \{p|_{\partial B} \mid p \in \mathcal{A}_\ell\}.$$

We have $\dim(\mathcal{H}_\ell) = \dim(\mathcal{A}_\ell) = 2\ell + 1$ in three spatial dimensions.

A standard orthonormal basis for \mathcal{H}_ℓ comprises the spherical harmonics of degree ℓ and order m , $\mathcal{B}_\ell = \{Y_\ell^m\}_{m \in \mathbb{Z}_\ell}$, given by

$$Y_\ell^m(\theta, \varphi) = \sqrt{\frac{2\ell+1}{4\pi} \frac{(\ell-m)!}{(\ell+m)!}} P_\ell^m(\cos(\theta)) e^{im\varphi}, \quad \ell \in \mathbb{N}_0, \quad m \in \mathbb{Z}_\ell,$$

where P_ℓ^m is an *associated Legendre polynomial* (with the Condon–Shortley phase). A symmetry condition is satisfied:

$$(3.1) \quad \overline{Y_\ell^m} = (-1)^m Y_\ell^{-m}.$$

The \mathcal{H}_ℓ -spaces are the eigenspaces for the Laplace–Beltrami operator $\Delta_{\partial B}$, with

$$(3.2) \quad \Delta_{\partial B} g = -\ell(\ell+1)g, \quad g \in \mathcal{H}_\ell.$$

Thus, there is the orthogonal decomposition

$$L^2(\partial B) = \bigoplus_{\ell=0}^{\infty} \mathcal{H}_\ell,$$

from which it holds that $\bigcup_{\ell=0}^{\infty} \mathcal{B}_\ell$ is an orthonormal basis for $L^2(\partial B)$ and $\bigcup_{\ell=1}^{\infty} \mathcal{B}_\ell$ is an orthonormal basis for $L_\diamond^2(\partial B)$.

Products of spherical harmonics have finite expansions in terms of spherical harmonics, and the Wigner $3j$ symbols, together with (3.1), can be used for computing the inner products (also called Gaunt coefficients) [13, section 34.3(vii), equation (34.3.22)],

$$(3.3) \quad \int_{\partial B} Y_{\ell_1}^{m_1} Y_{\ell_2}^{m_2} Y_{\ell_3}^{m_3} dS = G_{\ell_1, \ell_2, \ell_3}^{m_1, m_2, m_3},$$

with

$$(3.4) \quad G_{\ell_1, \ell_2, \ell_3}^{m_1, m_2, m_3} = \sqrt{\frac{(2\ell_1+1)(2\ell_2+1)(2\ell_3+1)}{4\pi}} \begin{pmatrix} \ell_1 & \ell_2 & \ell_3 \\ 0 & 0 & 0 \end{pmatrix} \begin{pmatrix} \ell_1 & \ell_2 & \ell_3 \\ m_1 & m_2 & m_3 \end{pmatrix}.$$

The integral in (3.3) vanishes if the following conditions are not met:

$$(3.5) \quad |\ell_1 - \ell_2| \leq \ell_3 \leq \ell_1 + \ell_2, \quad \sum_{j=1}^3 m_j = 0, \quad \text{and} \quad \sum_{j=1}^3 \ell_j \text{ is even.}$$

- (i) The first condition in (3.5) is known as the *triangle condition* for $3j$ symbols, and any $3j$ symbol vanishes if this condition is not met (see [13, section 34.2] and [15, section 2.1]).
- (ii) If the second condition in (3.5) is not met, then the second $3j$ symbol in (3.4) vanishes [13, section 34.2], although there are also other nontrivial zeros of this $3j$ symbol [15].
- (iii) When the triangle condition holds, the third condition in (3.5) is not met if and only if the first $3j$ symbol in (3.4) vanishes (see [13, section 34.3(i), equation (34.3.5)] and [15, equations (47) and (48)]).

One can combine (3.1) and (3.3) with the following lemma to give finite expansions in terms of spherical harmonics for the product of gradients of spherical harmonics. In the following, $\nabla_{\partial B}$ denotes a surface gradient on ∂B . As we have been unable to find the result published, we give a proof for the sake of completion.¹

¹The proof is inspired by ideas from a physics blog: <https://hyad.es/vsphint>.

LEMMA 3.1. Let $\ell_j \in \mathbb{N}_0$ and $g_{\ell_j} \in \mathcal{H}_{\ell_j}$ for $j \in \{1, 2, 3\}$. Then

$$\int_{\partial B} (\nabla_{\partial B} g_{\ell_1} \cdot \nabla_{\partial B} g_{\ell_2}) g_{\ell_3} \, dS = \frac{\ell_1(\ell_1 + 1) + \ell_2(\ell_2 + 1) - \ell_3(\ell_3 + 1)}{2} \int_{\partial B} g_{\ell_1} g_{\ell_2} g_{\ell_3} \, dS.$$

Proof. Below, ∇ denotes a gradient in B . We extend g_{ℓ_1} , g_{ℓ_2} , and g_{ℓ_3} to $B \setminus \{0\}$, constant in the radial direction. Using spherical coordinates gives

$$(3.6) \quad \nabla g_{\ell_i} \cdot \nabla g_{\ell_j} = r^{-2} \nabla_{\partial B} g_{\ell_i} \cdot \nabla_{\partial B} g_{\ell_j}$$

and, using (3.2),

$$(3.7) \quad \Delta g_{\ell_j} = r^{-2} \Delta_{\partial B} g_{\ell_j} = -r^{-2} \ell_j(\ell_j + 1) g_{\ell_j}.$$

In the computations below, one can replace B by $B \setminus B_\epsilon$ for an origin-centered ball B_ϵ with radius $\epsilon > 0$ and let $\epsilon \rightarrow 0$. Since the considered functions are integrable on B , the limiting process gives precisely the results below, so we avoid these unnecessary technicalities in what follows.

Define

$$(3.8) \quad E_{\ell_1, \ell_2, \ell_3} = \int_B (\nabla g_{\ell_1} \cdot \nabla g_{\ell_2}) g_{\ell_3} \, dx.$$

Consider the first integral on the right-hand side below: Integrating by parts, noting that the boundary term vanishes due to a vanishing normal derivative of g_{ℓ_2} , and using the product rule gives

$$(3.9) \quad E_{\ell_1, \ell_2, \ell_3} = - \int_B g_{\ell_1} (\Delta g_{\ell_2}) g_{\ell_3} \, dx - E_{\ell_2, \ell_3, \ell_1}.$$

Note that the assumptions needed for arriving at (3.9) are symmetric in terms of the indices ℓ_1, ℓ_2, ℓ_3 , and they can therefore be permuted to arrive at other such formulas. Thus, we may use the cyclic property (3.9) in the following way:

$$\begin{aligned} (3.10) \quad E_{\ell_1, \ell_2, \ell_3} &= - \int_B g_{\ell_1} (\Delta g_{\ell_2}) g_{\ell_3} \, dx - E_{\ell_2, \ell_3, \ell_1} \\ &= - \int_B g_{\ell_1} (\Delta g_{\ell_2}) g_{\ell_3} \, dx + \int_B g_{\ell_2} (\Delta g_{\ell_3}) g_{\ell_1} \, dx + E_{\ell_3, \ell_1, \ell_2} \\ &= - \int_B g_{\ell_1} (\Delta g_{\ell_2}) g_{\ell_3} \, dx + \int_B g_{\ell_2} (\Delta g_{\ell_3}) g_{\ell_1} \, dx - \int_B g_{\ell_3} (\Delta g_{\ell_1}) g_{\ell_2} \, dx - E_{\ell_1, \ell_2, \ell_3}. \end{aligned}$$

Combining (3.7) and (3.10) gives

$$\begin{aligned} E_{\ell_1, \ell_2, \ell_3} &= \frac{\ell_1(\ell_1 + 1) + \ell_2(\ell_2 + 1) - \ell_3(\ell_3 + 1)}{2} \int_B r^{-2} g_{\ell_1} g_{\ell_2} g_{\ell_3} \, dx \\ &= \frac{\ell_1(\ell_1 + 1) + \ell_2(\ell_2 + 1) - \ell_3(\ell_3 + 1)}{2} \int_{\partial B} g_{\ell_1} g_{\ell_2} g_{\ell_3} \, dS. \end{aligned}$$

The proof is concluded by using (3.6) and (3.8):

$$E_{\ell_1, \ell_2, \ell_3} = \int_{\partial B} (\nabla_{\partial B} g_{\ell_1} \cdot \nabla_{\partial B} g_{\ell_2}) g_{\ell_3} \, dS. \quad \square$$

3.2. On three-dimensional radial Zernike polynomials. Let R_ℓ^k be the three-dimensional radial Zernike polynomial

$$(3.11) \quad R_\ell^k(r) = \sqrt{2\ell + 4k + 3} \sum_{s=0}^k (-1)^s \binom{k}{s} \binom{\ell + 2k - s + \frac{1}{2}}{k} r^{\ell + 2k - 2s}, \quad \ell, k \in \mathbb{N}_0,$$

where the generalized binomial coefficient is

$$\binom{x}{n} = \frac{\Gamma(x+1)}{n! \Gamma(x-n+1)}, \quad x > n-1, \quad n \in \mathbb{N}_0.$$

In [14], the three-dimensional radial Zernike polynomials above are annotated as $R_{\ell+2k}^{(\ell)}$, similar to the two-dimensional radial Zernike polynomials in [10]. We have modified the notation to better fit with the spherical harmonics; however, one should keep this notational difference in mind.

For the next part, consider the Pochhammer symbol (rising factorial):

$$(x)_n = \frac{\Gamma(x+n)}{\Gamma(x)}, \quad x > 0, \quad n \in \mathbb{N}_0.$$

The coefficients in (3.11) are the same as those in [14]: Writing out the four binomial coefficients in [14], canceling recurring terms, and collecting some terms in Pochhammer symbols (using that $\Gamma(n+1) = n!$ for $n \in \mathbb{N}_0$) gives

$$\begin{aligned} & \frac{(-1)^s \sqrt{2\ell + 4k + 3}}{4^k} \binom{\ell + 2k}{\ell}^{-1} \binom{\ell + 2k}{s} \binom{\ell + k - s}{\ell} \binom{2\ell + 4k - 2s + 1}{2k} \\ &= \frac{(-1)^s \sqrt{2\ell + 4k + 3}}{k! 4^k} \binom{k}{s} \frac{(2\ell + 2k - 2s + 2)_{2k}}{(\ell + k - s + 1)_k}. \end{aligned}$$

Using the duplication formula for Pochhammer symbols [13, section 5.2(iii), equation (5.2.8)] (a consequence of the Legendre duplication formula for Γ -functions),

$$(2x)_{2k} = 4^k (x)_k \left(x + \frac{1}{2}\right)_k$$

combined with

$$\frac{(x)_k}{k!} = \binom{x + k - 1}{k}$$

gives the coefficients in (3.11).

The three-dimensional radial Zernike polynomials with the same index ℓ are orthonormal in the weighted space $L_{r^2}^2((0,1))$ [14, equation (33)]:

$$\langle R_\ell^k, R_\ell^{k'} \rangle_{L_{r^2}^2((0,1))} = \int_0^1 R_\ell^k(r) R_\ell^{k'}(r) r^2 dr = \delta_{k,k'}.$$

For $p \in \mathbb{N}_0$ there is the finite expansion (cf. [14, equations (39) and (40)] with the notational differences mentioned above in mind)

$$(3.12) \quad r^{\ell+2p} = \sum_{q=0}^p \chi_\ell^{p,q} R_\ell^q(r),$$

with

$$(3.13) \quad \chi_\ell^{p,q} = \langle r^{\ell+2p}, R_\ell^q \rangle_{L_{r^2}^2((0,1))} = \frac{\sqrt{2\ell + 4q + 3} (p - q + 1)_q}{(2\ell + 2p + 3) (\ell + p + \frac{5}{2})_q}$$

in terms of Pochhammer symbols.

PROPOSITION 3.2. $\{\psi_\ell^{k,m}\}_{\ell,k \in \mathbb{N}_0, m \in \mathbb{Z}_\ell}$ from (1.3) is an orthonormal basis for $L^2(B)$.

Proof. We have already argued that $\{\psi_\ell^{k,m}\}_{\ell,k \in \mathbb{N}_0, m \in \mathbb{Z}_\ell}$ is an orthonormal set in $L^2(B)$, so what remains is to prove density. Since $\{Y_\ell^m\}_{\ell \in \mathbb{N}_0, m \in \mathbb{Z}_\ell}$ is an orthonormal basis for $L^2(\partial B)$, it suffices to prove that r^n belongs to

$$\overline{\text{span}\{R_\ell^k \mid k \in \mathbb{N}_0\}}$$

for any $n, \ell \in \mathbb{N}_0$. By (3.12), we have that $r^{\ell+2p} \in \text{span}\{R_\ell^k \mid k \in \mathbb{N}_0\}$ for $p \in \mathbb{N}_0$. Hence, the proof reduces to approximating r^n in $L^2((0,1))$ by polynomials in $\text{span}\{r^{\ell+2p} \mid p \in \mathbb{N}_0\}$. This is possible by [10, Lemma 6.1]. \square

Note in particular that for $k=0$, $\{\psi_\ell^{0,m}\}_{\ell \in \mathbb{N}_0, m \in \mathbb{Z}_\ell}$ are the regular solid harmonics, the standard orthonormal basis for L^2 harmonic functions in B .

4. Proof of Theorem 1.1. For $\hat{\ell} \in \mathbb{N}$ and $\hat{m} \in \mathbb{Z}_{\hat{\ell}}$,

$$u_{\hat{\ell}}^{\hat{m}}(r, \theta, \varphi) = \frac{1}{\hat{\ell}} r^{\hat{\ell}} Y_{\hat{\ell}}^{\hat{m}}(\theta, \varphi)$$

is harmonic and has Neumann trace $Y_{\hat{\ell}}^{\hat{m}} \in L^2_\diamond(\partial B)$. Hence, for $\ell_j \in \mathbb{N}$ and $m_j \in \mathbb{Z}_{\ell_j}$ and by (3.1), we have in terms of the spherical coordinates

$$(4.1) \quad \nabla u_{\ell_1}^{m_1} \cdot \overline{\nabla u_{\ell_2}^{m_2}} = (-1)^{m_2} r^{\ell_1 + \ell_2 - 2} \left(Y_{\ell_1}^{m_1} Y_{\ell_2}^{-m_2} + \frac{1}{\ell_1 \ell_2} \nabla_{\partial B} Y_{\ell_1}^{m_1} \cdot \nabla_{\partial B} Y_{\ell_2}^{-m_2} \right).$$

By Lemma 3.1, (3.3), and the conditions in (3.5), the parenthesis at the end of (4.1) can be expanded by a *finite* number of spherical harmonics. In particular, (4.1) is in $L^2(B)$.

Now fix $\ell, k \in \mathbb{N}_0$ and $m \in \mathbb{Z}_\ell$. Since $\eta \in L^3(B) \subset L^2(B)$, there is an ℓ^2 -sequence of coefficients $c_{\ell'}^{k',m'}$, with $\ell', k' \in \mathbb{N}_0$ and $m' \in \mathbb{Z}_{\ell'}$, such that

$$\eta = \sum_{\ell', k' \in \mathbb{N}_0} \sum_{m' \in \mathbb{Z}_{\ell'}} c_{\ell'}^{k',m'} \psi_{\ell'}^{k',m'}.$$

The goal is to establish a direct formula for the coefficient $c_\ell^{k,m}$ in terms of $F\eta$ and coefficients with smaller k -indices.

We consider a particular choice of Neumann boundary conditions and use (1.2) and (4.1) to get

$$(4.2) \quad \langle (F\eta) Y_{k+1}^0, Y_{\ell+k+1}^m \rangle_{L^2(\partial B)} = - \int_B \eta \nabla u_{k+1}^0 \cdot \overline{\nabla u_{\ell+k+1}^m} dx = (-1)^{m+1} \int_B \eta r^{\ell+2k} \Phi_\ell^{k,m} dx,$$

with

$$\Phi_\ell^{k,m} = Y_{k+1}^0 Y_{\ell+k+1}^{-m} + \frac{1}{(k+1)(\ell+k+1)} \nabla_{\partial B} Y_{k+1}^0 \cdot \nabla_{\partial B} Y_{\ell+k+1}^{-m}.$$

Inserting the series for η into (4.2) gives

$$(4.3) \quad \begin{aligned} & \langle (F\eta) Y_{k+1}^0, Y_{\ell+k+1}^m \rangle_{L^2(\partial B)} \\ &= (-1)^{m+1} \sum_{\ell', k' \in \mathbb{N}_0} \sum_{m' \in \mathbb{Z}_{\ell'}} c_{\ell'}^{k',m'} \langle r^{\ell+2k}, R_{\ell'}^{k'} \rangle_{L^2_{r^2}((0,1))} \int_{\partial B} \Phi_\ell^{k,m} Y_{\ell'}^{m'} dS. \end{aligned}$$

Remark 4.1. A subtle but important point is that F is continuous with respect to $L^3(B)$, so the integral in (1.2) is a dual pairing between $L^3(B)$ for η and $L^{3/2}(B)$ for the product of gradients. But the series for η converges in $L^2(B)$. Choosing the Neumann conditions to be spherical harmonics is therefore essential such that (4.1) is in fact an $L^2(B)$ -function, as we argued above. This implies that the integral instead acts as the $L^2(B)$ inner product, which, by continuity, enables that the summation can be moved outside the integral in (4.3).

It may well be that if $\eta \in L^3(B)$, then the series also converges in $L^3(B)$; such a result, e.g., holds for Fourier series, with convergence in L^p for functions in L^p with $p \in (1, \infty)$. However, we prefer to avoid what is likely a technical endeavor of proving such a result.

Lemma 3.1 gives

$$(4.4) \quad \int_{\partial B} \Phi_{\ell}^{k,m} Y_{\ell'}^{m'} dS = \tau_{\ell,\ell'}^k \int_{\partial B} Y_{k+1}^0 Y_{\ell+k+1}^{-m} Y_{\ell'}^{m'} dS,$$

with

$$(4.5) \quad \begin{aligned} \tau_{\ell,\ell'}^k &= 1 + \frac{(k+1)(k+2) + (\ell+k+1)(\ell+k+2) - \ell'(\ell'+1)}{2(k+1)(\ell+k+1)} \\ &= \frac{(\ell+2k+2-\ell')(\ell+2k+3+\ell')}{2(k+1)(\ell+k+1)}. \end{aligned}$$

From (3.5), (4.4) vanishes unless $m' = m$. It also vanishes unless $\ell+2k+2+\ell'$ is even; i.e., $\ell+\ell'$ must be even. Finally, we need $\ell \leq \ell' \leq \ell+2k+2$ and actually $\ell \leq \ell' \leq \ell+2k$ because $\tau_{\ell,\ell'}^k = 0$ for $\ell' = \ell+2k+2$ and $\ell+\ell'$ is odd for $\ell' = \ell+2k+1$. This reduces to the cases

$$m' = m \quad \text{and} \quad \ell' = \ell + 2s, \quad s \in \{0, \dots, k\}.$$

Hence, using these indices and (3.3) simplifies (4.3) to

$$(4.6) \quad \langle (F\eta) Y_{k+1}^0, Y_{\ell+k+1}^m \rangle_{L^2(\partial B)} = \sum_{k' \in \mathbb{N}_0} \sum_{s=0}^k c_{\ell+2s}^{k',m} \langle r^{\ell+2k}, R_{\ell+2s}^{k'} \rangle_{L_{r^2}^2((0,1))} D_{\ell,s}^{k,m},$$

with

$$(4.7) \quad D_{\ell,s}^{k,m} = (-1)^{m+1} \tau_{\ell,\ell+2s}^k G_{k+1,\ell+k+1,\ell+2s}^{0,-m,m}.$$

Writing $r^{\ell+2k} = r^{\ell+2s+2(k-s)}$ for $s \in \{0, \dots, k\}$ implies that we can use (3.12) to write

$$r^{\ell+2k} = \sum_{q=0}^{k-s} \chi_{\ell+2s}^{k-s,q} R_{\ell+2s}^q(r).$$

By orthonormality of $R_{\ell+2s}^{k'}$ and $R_{\ell+2s}^q$, their inner products vanish unless $k' = q$, which from (4.6) gives

$$\langle (F\eta) Y_{k+1}^0, Y_{\ell+k+1}^m \rangle_{L^2(\partial B)} = \sum_{s=0}^k \sum_{q=0}^{k-s} \chi_{\ell+2s}^{k-s,q} D_{\ell,s}^{k,m} c_{\ell+2s}^{q,m} = \sum_{q=0}^k \sum_{s=0}^{k-q} \chi_{\ell+2s}^{k-s,q} D_{\ell,s}^{k,m} c_{\ell+2s}^{q,m},$$

where the summation indices could be swapped, as it corresponds to summing over the same triangular pairs of indices. Writing

$$(4.8) \quad Q_{\ell,s}^{k,m,q} = \chi_{\ell+2s}^{k-s,q} D_{\ell,s}^{k,m}$$

thus gives the formula

$$c_{\ell}^{k,m} = (Q_{\ell,0}^{k,m,k})^{-1} \left(\langle (F\eta) Y_{k+1}^0, Y_{\ell+k+1}^m \rangle_{L^2(\partial B)} - \sum_{q=0}^{k-1} \sum_{s=0}^{k-q} Q_{\ell,s}^{k,m,q} c_{\ell+2s}^{q,m} \right).$$

Of course, we need to verify that $Q_{\ell,0}^{k,m,k} \neq 0$ for all $\ell, k \in \mathbb{N}_0$ and $m \in \mathbb{Z}_{\ell}$. Going backward from (4.8), (4.7), (4.5), and (3.13), we have

$$(4.9) \quad \begin{aligned} Q_{\ell,s}^{k,m,q} &= (-1)^{m+1} \chi_{\ell+2s}^{k-s,q} \tau_{\ell,\ell+2s}^k G_{k+1,\ell+k+1,\ell+2s}^{0,-m,m} \\ &= (-1)^{m+1} \frac{\sqrt{2\ell+4q+4s+3}(k-s+1)(k-q-s+1)_q}{(k+1)(\ell+k+1)(\ell+k+s+\frac{5}{2})_q} G_{k+1,\ell+k+1,\ell+2s}^{0,-m,m}. \end{aligned}$$

Since $s \leq k-q \leq k$, the only possibility for (4.9) to vanish is related to the Gaunt coefficient. Since the conditions in (3.5) are satisfied, we have already argued after (3.5) that the only possibility for getting a zero is in the last of the $3j$ symbols in (3.4). For $G_{k+1,\ell+k+1,\ell}^{0,-m,m}$ (with $s=0$), the corresponding $3j$ symbol is

$$(4.10) \quad \begin{pmatrix} k+1 & \ell+k+1 & \ell \\ 0 & -m & m \end{pmatrix} = \begin{pmatrix} \ell & k+1 & \ell+k+1 \\ m & 0 & -m \end{pmatrix}.$$

Here we used [13, section 34.3(ii), equation (34.3.8)] that $3j$ symbols are invariant to even permutations of the columns. For the latter $3j$ symbol in (4.10), [13, section 34.3(i), equation (34.3.6)] and $|m| \leq \ell$ imply that it is indeed nonzero, hence concluding the proof of Theorem 1.1. \square

Appendix A. Extension of the linearized problem. In this appendix, we consider a bounded smooth domain Ω in \mathbb{R}^d for integer $d \geq 2$. Replacing B with Ω in the conductivity equation (1.1), the corresponding ND map $\Lambda(\gamma)$ is a compact self-adjoint operator in $\mathcal{L}(L_{\diamond}^2(\partial\Omega))$, and $\gamma \mapsto \Lambda(\gamma)$ is Fréchet differentiable with respect to complex-valued perturbations $\eta \in L^{\infty}(\Omega)$.

For $F = D\Lambda(1; \eta)$, the Fréchet derivative of Λ at $\gamma \equiv 1$ with respect to perturbation η , $F \in \mathcal{L}(L^{\infty}(\Omega), \mathcal{L}(L_{\diamond}^2(\partial\Omega)))$ with

$$(A.1) \quad \langle (F\eta)f, g \rangle_{L^2(\partial\Omega)} = - \int_{\Omega} \eta \nabla u_f \cdot \overline{\nabla u_g} \, dx,$$

where u_f and u_g are harmonic functions in Ω with f and g as their Neumann traces, respectively.

PROPOSITION A.1. *F extends via (A.1) to an operator in $\mathcal{L}(L^d(\Omega), \mathcal{L}(L_{\diamond}^2(\partial\Omega)))$.*

Proof. The proof is analogous to that of [10, Proposition 1.1]. Let $\eta \in L^d(\Omega)$ and $f, g \in L_{\diamond}^2(\partial\Omega)$. According to [12, Chapter 2, Remark 7.2], $u_f, u_g \in H^{3/2}(\Omega)/\mathbb{C}$ with continuous dependence on the Neumann data, i.e.,

$$(A.2) \quad \|u_f\|_{H^{3/2}(\Omega)/\mathbb{C}} \leq C \|f\|_{L^2(\partial\Omega)} \quad \text{and} \quad \|u_g\|_{H^{3/2}(\Omega)/\mathbb{C}} \leq C \|g\|_{L^2(\partial\Omega)}.$$

Using the continuous embedding $H^{1/2}(\Omega) \hookrightarrow L^{\frac{2d}{d-1}}(\Omega)$ (e.g., [5, Corollary 4.53]) and the generalized Hölder inequality, we may estimate as follows:

$$\begin{aligned} |\langle (F\eta)f, g \rangle_{L^2(\partial\Omega)}| &= \left| \int_{\Omega} \eta \nabla u_f \cdot \overline{\nabla u_g} \, dx \right| \\ &\leq \|\eta\|_{L^d(\Omega)} \|\nabla u_f\|_{L^{\frac{2d}{d-1}}(\Omega)} \|\nabla u_g\|_{L^{\frac{2d}{d-1}}(\Omega)} \\ &\leq C \|\eta\|_{L^d(\Omega)} \|\nabla u_f\|_{H^{1/2}(\Omega)} \|\nabla u_g\|_{H^{1/2}(\Omega)} \\ &\leq C \|\eta\|_{L^d(\Omega)} \|u_f\|_{H^{3/2}(\Omega)/\mathbb{C}} \|u_g\|_{H^{3/2}(\Omega)/\mathbb{C}}. \end{aligned}$$

Combining this with (A.2) concludes the proof. \square

Acknowledgments. We thank Nuutti Hyvönen (Aalto University) for useful discussions on the method and its differences to the corresponding two-dimensional method.

REFERENCES

- [1] A. ALLERS AND F. SANTOSA, *Stability and resolution analysis of a linearized problem in electrical impedance tomography*, Inverse Problems, 7 (1991), pp. 515–533, <https://doi.org/10.1088/0266-5611/7/4/003>.
- [2] S. AXLER, P. BOURDON, AND W. RAMEY, *Harmonic Function Theory*, Springer-Verlag, Berlin, 2001.
- [3] A. AUTIO, H. GARDE, M. HIRVENSALO, AND N. HYVÖNEN, *Linearization-based direct reconstruction for EIT using triangular Zernike decompositions*, Inverse Probl. Imaging, 19 (2025), <https://doi.org/10.3934/ipi.2024040>.
- [4] A. P. CALDERÓN, *On an inverse boundary value problem*, in Seminar on Numerical Analysis and Its Applications to Continuum Physics, Sociedade Brasileira de Matemática, Rio de Janeiro, Brazil, 1980, pp. 65–73.
- [5] F. DEMENGEL AND G. DEMENGEL, *Functional Spaces for the Theory of Elliptic Partial Differential Equations*, Springer-Verlag, Berlin, 2012, <https://doi.org/10.1007/978-1-4471-2807-6>.
- [6] C. EFTHIMIOU AND C. FRYE, *Spherical Harmonics in p Dimensions*, World Scientific, River Edge, NJ, 2014, <https://doi.org/10.1142/9134>.
- [7] D. DOS SANTOS FERREIRA, C. E. KENIG, J. SJÖSTRAND, AND G. UHLMANN, *On the linearized local Calderón problem*, Math. Res. Lett., 16 (2009), pp. 955–970, <https://doi.org/10.4310/MRL.2009.v16.n6.a4>.
- [8] D. DOS SANTOS FERREIRA, Y. KURYLEV, M. LASSAS, T. LIIMATAINEN, AND M. SALO, *The linearized Calderón problem in transversally anisotropic geometries*, Int. Math. Res. Not., 2020 (2020), pp. 8729–8765, <https://doi.org/10.1093/imrn/rny234>.
- [9] H. GARDE AND N. HYVÖNEN, *Series reversion in Calderón’s problem*, Math. Comp., 91 (2022), pp. 1925–1953, <https://doi.org/10.1090/mcom/3729>.
- [10] H. GARDE AND N. HYVÖNEN, *Linearized Calderón problem: Reconstruction and Lipschitz stability for infinite-dimensional spaces of unbounded perturbations*, SIAM J. Math. Anal., 56 (2024), pp. 3588–3604, <https://doi.org/10.1137/23M1609270>.
- [11] T. GUSTAFSSON AND G. D. MCBAIN, *scikit-fem: A Python package for finite element assembly*, J. Open Source Softw., 5 (2020), 2369, <https://doi.org/10.21105/joss.02369>.
- [12] J.-L. LIONS AND E. MAGENES, *Non-Homogeneous Boundary Value Problems and Applications*, Vol. 1, Springer-Verlag, Berlin, 1972, <https://doi.org/10.1007/978-3-642-65161-8>.
- [13] D. W. LOZIER, B. I. SCHNEIDER, R. F. BOISVERT, C. W. CLARK, B. R. MILLER, B. V. SAUNDERS, H. S. COHL, F. W. J. OLVER, A. B. OLDE DAALHUIS, AND M. A. MCCLAIN, eds., *NIST Digital Library of Mathematical Functions*, National Institute of Standards and Technology, U.S. Department of Commerce, Washington, DC, <https://dlmf.nist.gov>, accessed March 2024.
- [14] R. J. MATHAR, *Zernike basis to Cartesian transformations*, Serb. Astron. J., 179 (2009), pp. 107–120, <https://doi.org/10.2298/SAJ0979107M>.
- [15] J.-C. PAIN, *Some properties of Wigner 3j coefficients: Non-trivial zeros and connections to hypergeometric functions*, Eur. Phys. J. A, (2020), 296, <https://doi.org/10.1140/epja/s10050-020-00303-9>.

- [16] V. SHARAFUTDINOV, *Linearized inverse problem for the Dirichlet-to-Neumann map on differential forms*, Bull. Sci. Math., 133 (2009), pp. 419–444, <https://doi.org/10.1016/j.bulsci.2008.07.001>.
- [17] J. SJÖSTRAND AND G. UHLMANN, *Local analytic regularity in the linearized Calderón problem*, Anal. PDE, 9 (2016), pp. 515–544, <https://doi.org/10.2140/apde.2016.9.515>.
- [18] F. ZERNIKE, *Beugungstheorie des schneidenverfahrens und seiner verbesserten form, der phasenkontrastmethode*, Physica, 1 (1934), pp. 689–704, [https://doi.org/10.1016/S0031-8914\(34\)80259-5](https://doi.org/10.1016/S0031-8914(34)80259-5).